Journal of Mechanical Engineering and Sciences
ISSN (Print): 2289-4659; e-ISSN: 2231-8380
Volume 13, Issue 4, pp. 6036-6058, December 2019

DOI: https://doi.org/10.15282/jmes.13.4.2019.21.0477

Design and numerical analysis of an efficient H-Darrieus vertical-axis hydrokinetic turbine

Ramírez D[1], Rubio-Clemente A[1,2], Chica E[1]

[1] Departamento de Ingeniería Mecánica, Facultad de Ingeniería,
Universidad de Antioquia UdeA, Calle 70 No. 52-21, Medellín, Colombia.
Email: edwin.chica@udea.edu.co
Phone: +5742198553
[2] Facultad de Ingeniería, Tecnológico de Antioquia–Institución Universitaria TdeA,
Calle 78b, No. 72A-220, Medellín, Colombia.

ABSTRACT

Hydrokinetic turbines are one of the technological alternatives to generate and supply electricity for rural communities isolated from the national electrical grid with almost zero emission. The Darrieus turbine is one of the options that can be used as a hydrokinetic turbine due to its high power coefficient (C_p) and easy manufacture. In the present work, the design and hydrodynamic analysis of a Darrieus vertical-axis hydrokinetic turbine of 500 W was carried out. A free stream velocity of 1.5 m/s was used for the design of the blades. The diameter (D) and blade length (H) of the turbine were 1.5 m and 1.13 m, respectively. The blade profile used was NACA0025 with a chord length of 0.33 m and solidity (σ) of 0.66. Two (2D) and three dimensional (3D) numerical analyses of the unsteady flow through the blades of the turbine were performed using ANSYS Fluent version 18.0, which is based on a Reynolds-Averaged Navier-Stokes (RANS) model. A transient 2D simulation was conducted for several tip speed ratios (TSR) using a k-ω Shear Stress Transport turbulence (SST) scheme. The optimal TSR was found to be around 1.75. Main hydrodynamic parameters, such as torque (T) and C_P, were investigated. Additionally, 3 geometrical configurations of the turbine rotor were studied using a 3D numerical model in order to identify the best configuration with less C_p and T fluctuation. The maximum C_p average was 0.24 and the amplitude of C_p variation, near 0.24 for the turbine model with 3 blades of H equal to 1.13 m. On the other hand, for the turbine models with 6 and 9 blades of H equal to 0.565 m and 0.377 m, respectively, the maximum C_p averages were 0.51 and 0.55, respectively, and the amplitude of C_p variation, near 0.07 for the model with 6 blades and 0.17 for the model with 9 blades. This revealed that the hydrokinetic turbine with a geometrical configuration of 6 blades greatly improves the performance of the turbine due to this model has advantages compared to models with 3 and 9 blades, in terms of the reduction of their T curve fluctuation.

Keywords: Darrieus hydrokinetic turbine; numerical simulation; power coefficient; tip speed ratio.

INTRODUCTION

Hydrokinetic turbines convert the kinetic energy of river or marine currents into mechanical or electrical power. In this regard, hydrokinetic turbines can be considered as an alternative for the generation of decentralized clean electrical power from renewable resources and could be used in regions where topographical and geographical conditions become main obstacles for the centralized power distribution system [1-2]. Additionally, this technology can be easily adopted and efficiently run without interferring with the natural course of rivers, reducing the environmental impact related to the store of the potential energy in artificial reservoirs by means of the use of water dams [1-4]. Additionally, hydrokinetic turbines can be moved to another location or entirely removed from the water current [1-4].

This type of turbines have horizontal, vertical or inclined axes of rotation, whose function is similar to wind turbines, capturing energy through hydrodynamic processes generated from lift and drag forces on the turbine blades [5-7]. The vertical-axis cross-flow hydrokinetic turbines have the axis of rotation perpendicular to the free-stream and it rotates due to the lift force or drag generated in the blades when subjected to the water flow [5-7]. Guney and Kaygusuz [8] carried out a study for a detailed comparison of various types of hydrokinetic turbines and concluded that a vertical-axis turbine is more suitable for the cases where water flow rate is relatively limited. Authors also reported that horizontal-axis turbines have higher efficiency and ability to self-start; however, this kind of turbines has higher manufacturing and transportation costs associated. Because of their high-efficiency, axial flow turbines are mainly used in ocean and tidal applications [3,5,6,8]. Therefore, vertical-axis turbines are generally used for small scale power generation because they are less expensive, cause less impact on the aquatic life due to their reduced rotational speed and larger internal empty space, and require less maintenance compared to horizontal-axis hydrokinetic turbines. Furthermore, vertical-axis turbines generate power in spite of the direction of the flowing medium and the electric generator can be mounted above water level, which allows them for an easy maintenance [6,8,9]. In fact, vertical-axis turbines are designed so that the direction of rotation is always the same, independently on the flow direction.

The Savonius turbines, helical turbines (also known as Gorlov turbines), Darrieus turbines and H-shaped Darrieus turbines are vertical-axis turbines [10]. The Gorlov turbine has helically shaped blades which are more complicated to be manufactured [11] in contrast to the H-Darrieus turbine, whose straight blades are easier to be constructed; however, the H-Darrieus turbine has some problems including self-starting resonant at a particular rotational speed, poor starting torque and torque fluctuations, or torque ripple of the turbine due to blades passing in and out of torque-generating regions [6,10,11]. These cyclical loads are of concern when designing for turbine reliability and longevity. To avoid these disadvantages, different hydrofoil profiles, helical blade configurations (the helicity is provided to increase the starting torque (T) and to reduce T fluctuation during rotation [12]) and the increase in the number of blades with variable pitch might be used to reduce shaking of the blades while maintaining strong starting torque and high peak power coefficient (C_p) [13]. On the other hand, the Savonius turbine, even though it can be constructed easily, it has very low efficiency in comparison with the other types of vertical-axis turbines [14-15]. Indeed, the Darrieus rotor has about an efficiency of 57% higher than that of a Savonius rotor [16-17].

It is important to note that the technology of vertical-axis hydrokinetic turbines is still in its emerging stage; therefore, some researches have been focused on the efficient design, fabrication and testing of this hydrokinetic turb ine. In addition, due to the high cost of the harvesting energy of water current by these turbines, choosing a turbine with an optimum performance at the selected site is an aspect of crucial interest [18]. Many researchers have conducted experimental and numerical investigations into current turbine design [16-19]. In general, the studies show that the performance of the Darrieus turbine is strongly dependent on the type of the blade used and other parameters, such as velocity of the water flow (V), tip speed ratio (TSR), number of blades (N), solidity (σ) and aspect ratios (AR). For example, to design a duct in order to know its effect on the power output of a H-Darrieus turbine, a Computational Fluid Dynamics (CFD) analysis was carried out by Malipeddi and Chatterjee [19]. Authors designed a duct which was capable of reducing T variations and increasing C_p from 0.4 to 0.64. The results revealed the performance of a H-Darrieus turbine using an appropriately designed duct.

In turn, Tanaka et al. [20], designed and investigated the performance of a Darrieus rotor under overflow and bypass conditions and when a waste screening system was installed to avoid floating waste. It was found that the waste screening system was effective with bypass flow rate, although the efficiency was lost.

On the other hand, the performance of two variable pitch straight blade vertical-axis hydrokinetic turbines, one in open water and other one in a laboratory towing tank, was modeled and measured experimentally by Kirke [21]. 2D modeling, ignoring parasitic drag losses, over-predicts peak C_p for turbines with simple sinusoidal pitch at around 45% and up to 49% for an optimized cam-driven pitch regime. The relation of struts shape and Reynolds number with C_p was determined using laboratory experiments with a H-Darrieus turbine that had tapered blades (σ varying from 0.12 to 0.07) by Bachant et al. [22]. Authors observed that using cylindrical struts increases drag, which resulted in adverse effects on the turbine performance; hence they used NACA0021 to reduce drag. Bachant and coworkers also found that a TRS of 5 caused a performance decrease of 5% since struts drag increased even if streamline struts are used. In addition, the C_p achieved showed linear relation with Reynolds number, while its value decreased as TSR value was increased beyond 3.1. A peak C_p equal to 0.37 and a rotor drag coefficient (CD) equal to 0.84 were observed at a TRS of 3.1 and Reynolds number of 1.3e6.

Furthermore, Bachant and Wosnik studied the effect of Reynolds number and wake characteristics on performance of a large laboratory-scale high σ cross-flow turbine [23]. They found that the performance of a high σ (c/R=0.28) cross-flow turbine becomes essentially Re-independent at a Reynolds number based on the turbine diameter ReD ≈1e6 or an approximate Reynolds number based on the blade chord Rec≈ 2e5. Authors also proposed a model to predict the Reynolds number dependence of a vertical-axis water rotor by approximating its performance and wake characteristics once its diameter has reached at 1e6 Reynolds number.

The performance and flow evaluation for a low-speed hydrokinetic turbine of Darrieus type, operating in a confined flow channel was presented by Gorle et al., in 2016 [24]. The investigation methods included computations (2D CFD) using Chimera meshes and experiments (2D-2C PIV), including phase-locked measurements. k-ω Shear Stress Transport turbulence (SST) model based numerical results for velocity fields, instantaneous vortex dynamics, wake geometry and Q-criterion were validated using experimental findings.

In turn, Gosselin et al. [25] performed a detailed 2D and 3D CFD analyses of a Darrieus wind turbine to study all the major factors affecting the turbine performance; i.e., TSR, Reynolds number, σ, N, AR, pitch angle (θ) and blade thickness. They also mentioned that for high-Reynolds applications, optimal radius-based σ is found to be around σ =0.2, while higher solidities show a lower maximum efficiency than what was previously published using simpler streamtube based methods [25].

A detailed discussion about the effect of various design parameters, including σ and the type of hydrofoil on the performance of a Darrieus type hydrokinetic turbine, was reported in detail by Patel et al. [26]. The experiments with hydrofoil NACA0015 and NACA0018 demonstrated the highest C_p with a value equal to 0.15 at a σ of around 0.382. Further experiments to evaluate the effect of spanwise and streamwise distance on the performance of a Darrieus turbine were investigated for its application as hydrofarm. A minimum distance of 7- and 3-fold the rotor diameter along the streamwise and spanwise direction, respectively, was found to be essential in a hydrofarm using Darrieus turbines.

Experiments conducted by Somoano and Huera-Huarte [27], with a 3-straight bladed cross-flow turbine allowed explaining the performance differences in this type of turbines as a function of the operational TSR. Authors showed the necessity of conducting analyses of the vortex dynamics inside the rotor in order to explain the physical mechanisms leading to the performance change. These authors [28] also analyzed the variations in flow dynamics inside the rotor of a 3-straight-bladed cross-flow turbine for different blade pitches using a turbine model based on symmetric NACA0015 profiles with a chord-to-diameter ratio of 0.16. Authors showed how a θ of 8° toe-out resulted in the highest performance curves. They also proposed a new equation for the angle of attack (α) as a function of the azimuthal position after detailed measurements of the local velocities around the blades.

Experimental investigations of a Darrieus type straight blade hydroturbine were carried out and the effects of parameters, such as σ, N, chord length and V, on the turbine performance were checked by Patel et al. [29]. In numerical study, 3 non-cambered NACA blade profiles were analyzed and concluded that power mainly depends on the blade profile. For low-speed turbines, NACA0021 gave the maximum C_p for all the tested profiles. From 5 experimental trials of the Darrieus hydroturbine in a water channel with a NACA0021 blade profile of 0.8 σ, turbine self-starting was obtained. It was found that as σ is increased, a better self-starting capability of the turbine is observed. Additionally, maximum power was found to be only achieved at higher σ and V with lower TSR. Furthermore, as N increased more than 3, then C_p is decreased.

Recently, Patel et al. [30] concluded that the performance of a Darrieus turbine was enhanced using a blocking plate optimally located at the upstream side of the retarding vane. The C_p of a turbine without blocking plate was enhanced from 0.125 to 0.36 by using an optimized blocking plate width and location.

In the literature, studies related to the determination of the relation of 3D geometrical configuration of the blades, as proposed in this work, with the turbine performance, are not reported from the authors' knowledge. Additionally, it is highlighted that Darrieus turbines are not extensively used [2, 3, 6, 8] due to their poor self-starting characteristics and high T fluctuation. Under this scenario, in order to improve the technology for energy extraction using a H-Darrieus turbine, numerical simulations are proposed in order to study the flow field around the turbine blades and analyze different turbine design parameters for providing an optimal configuration before to proceed with the turbine manufacture. The influences of

N and TSR on T, C_p and fluctuation of these parameters are verified to define the best configuration regarding the efficiency and costs associated with the application of this technology in isolated regions.

MATERIALS AND METHODS

Design of the Vertical-axis Hydrokinetic Turbine

The rotor is the most important component in a hydrokinetic turbine. It is designed to capture water energy and convert it into rotating mechanical energy. The geometry and dimension of the rotor is determined by the performance requirements of the hydrokinetic turbine. In general, two fundamental issues must be considered simultaneously in rotor design process: hydrodynamic performance and structural design. The hydrodynamic characteristics of the turbine are influenced by the selected hydrofoil [6, 7, 31, 32].

The design methods of the main characteristics of the turbine rotor are based on the same incompressible flow techniques used for designing wind turbines. The first step involved in the rotor design is to fix the turbine output power (P) and estimate the turbine diameter (D) and blade length (H). For this purpose, as widely known in the literature, the energy in moving water is in the form of kinetic energy. In this sense, the power (P) available from the water is proportional to water density (ρ), area of the water being considered (S_{ref}), and V [15, 16]. The relationship between the variables mentioned above is provided in Equation. (1).

$$P = \frac{1}{2}\rho S_{ref} V^3 \tag{1}$$

A hydrokinetic turbine cannot extract 100% of the water energy because some of the water energy is used in pressure change occurring across the turbine blades. This pressure change causes a decrease in velocity and, therefore, in the usable energy. Thus, Equation (1) gives the ideal power in a fluid flow. However, hydrokinetic turbines are limited by blade efficiencies, mechanical losses in transmissions, electrical losses and by the theoretical amount of energy allowed to be extracted from water [31-32]. Because of these losses and inefficiencies, two more variables are added to Equation (1). The first variable is η, which is a measure of the efficiency of the gearbox, the electrical inverter and the generator. It takes into account all the friction, slippage and heat losses associated with the interior mechanical and electrical components. Values for η can greatly differ among the turbine models. Some smaller turbines do not have transmission; therefore, the electric generator is directly moved by the turbine shaft, while larger turbines have transmission and reasonably involved inverters and synchronizing gear [33]. The range of values of η are presented in the literature, highlighting the study conducted by Hangerman et al., which states a range of efficiencies between 95% and 98%. However, for the design of the blade, a reasonable and conservative value of η around 70% was used in this work [34].

The second variable is C_p. C_p is a measure of the blade or hydrofoil efficiency. It takes into account the hydrofoil shape and the hydrodynamic forces of lift and drag. C_p expresses the hydrofoil ability to transform the water kinetic energy into mechanical power which is delivered to a turbine transmission or generator. A higher C_p is preferred over a lower C_p value. These C_p values vary with the turbine size and depend on the water speed, rotational

speed of the turbine and blade parameters such as θ and α [6, 34-36]. The pitch angle for a horizontal-axis hydrokinetic turbine is the angle between the blade motion and the chord line of the blade [31, 32]; whereas for a vertical-axis hydrokinetic turbine θ is between the line perpendicular to the blades motions and the chord line of the blade. In turn, α is the angle between the relative water velocity and the centreline of the blade. For fixed pitch turbine, these angles do not change and C_p is directly related to TSR, also expressed as λ. A C_p equal to 59.3% can be considered in the case of an ideal turbine; however; an ideal turbine is a theoretical case. C_p in the range of 25-40% are very good, and this is the case for most large-scale turbines. The maximization of the C_p is of fundamental importance in order to optimize the extraction of energy from water [35, 36].

Placing these two variables, η and C_p into Equation. (1), Equation. (2) is obtained.

$$P = \frac{1}{2}\rho S_{ref} V^3 C_p \eta \tag{2}$$

Equation. (2) is considered the power equation for hydrokinetic turbine. P is the net power derived from the water after accounting for losses and inefficiencies. In Equation (2), the area S_{ref} refers to the swept area of a turbine. For a H-Darrieus vertical-axis hydrokinetic turbine, this area depends on both D and H [36, 37]. Therefore, the area is given by Equation. (3).

$$S_{ref} = DH = 2RH \tag{3}$$

In general, the performance of a rotor turbine is governed by the following parameters: blade profile and chord (C); N; σ, based on the turbine radius (R); TSR; blade AR and blade configuration (including straight and helix blades, among others). In relation to blade profile, there are a great number of hydrofoil families and thicknesses which might be suitable for Darrieus turbines. Since it is impossible to analyze all of them, the choices must be narrowed in some way. Symmetrical hydrofoils have been chosen traditionally because energy capture is approximately symmetrical about the turbine axis. In this sense, the majority of the previously conducted research activities on vertical-axis hydrokinetic turbines were focused on straight bladed vertical hydrokinetic turbines equipped with symmetric hydrofoils (such as NACA 4-digit series of 0012, 0015, 0018, 0025). In this work, the profile NACA 0025 was selected [35, 36, 38]. The maximum C_p of a turbine with profile NACA 0025 was examined numerical and experimentally by Dai and Lam [38]. The results showed that a maximum average C_p as 25.1% was obtained for a TSR as 1,745. This value of C_p was used for the design of the blade. C is the length between the leading and trailing edge of the blade profile. The blade thickness and shape are determined by the hydrofoil used, where the blade curvature and maximum thickness are defined as percentage of the chord. The parameter N has a direct effect on the smoothness of rotor operation as it can compensate cycled hydrodynamic loads [6, 36, 37]. For easiness of building, 3 blades have been considered for the design of the rotor. In general, 3 blades are used for the turbine system to keep the dynamic balance and minimize the fatigue effect. In turn, σ is defined as the ratio between the total blade area and the projected turbine area [36, 37]. It is an important non-dimensional parameter which affects self-starting capabilities and for straight bladed hydrokinetic turbine is calculated from Equation. (4).

$$\sigma = \frac{NC}{2R} \tag{4}$$

On the other hand, λ is the ratio of the speed of the blade, at its tip, to the speed of the flowing water. This ratio has a strong influence on the efficiency of the turbine [31, 32, 35]. TSR of a hydrokinetic turbine is defined as Equation. (5).

$$\lambda = \frac{R\omega}{V} \tag{5}$$

where ω is the rotational speed of the rotor of the hydrokinetic turbine (rad/s). Each rotor design has an optimal TSR at which the maximum power extraction is achieved. The rotor AR is defined as the ratio between the blade length and the turbine R [36, 37]. It can be defined as represented by Equation. (6).

$$AR = \frac{H}{R} \tag{6}$$

The optimum range for the rotor AR for the vertical-axis wind turbine was obtained using the double-multiple streamtube (DMS) analytical approach by Mojtaba et al., [37] and it was found to be $1 < \frac{H}{R} < 4$. The hydrokinetic turbine was designed for a rotor with an AR of 1.5. Nevertheless, before using Equation (2), V must be determined or assumed. In this work, assuming that V is 1.5 m/s because it is an average speed of the great rivers of Colombia, P is 500 W, η is 70% and ρ is 997 kg/m^3 (25 °C); R and H were calculated. In this study, H and R were equal to 1.13 m and 0.75 m, respectively. Long blades can cause many natural frequency of vibration, which must be avoided during the operation [4-6].

Subsequently, given the rotor design parameters (e.g., R, TSR, hydrofoil and water current velocity, among others), the main task of the blade design is to determine C, which can be obtained by equaling the thrust on the rotor determined from the momentum theory with the thrust obtained from the blade element theory, considering the drag different of zero [5, 31]. Therefore, C can be worked out using Equation. (7).

$$C = \frac{8aRsin^2\alpha}{(1-a)sin^2\theta(C_D cos(\alpha-\theta) - C_L sin(\alpha-\theta))} \tag{7}$$

where a is the axial induction factor that is defined as the fractional decrease in the water velocity between the free stream and the rotor plane. θ is the azimuth angle, and α is the angle of attack. On the other hand, C_L is the lift coefficient and C_D, the drag coefficient that depend on the shape of the blade and Reynolds number under a given operating condition. C_L refers to the dynamic lift characteristics of a 2D foil section, with the reference area replaced by the foil chord. In turn, C_D is a dimensionless quantity that is used to quantify the drag or resistance of an object in fluid environment. The values of C_L (0.5097) and C_D (0.0092) were used. α, a variable in Equation. (7) can also be found from test data, which in this case was 5° [35]. The value of axial induction factor can be determined from Equation. (8) that relates the C_p with axial induction factor (a). Therefore, for a C_p equal to 0.25 and η equal to 70%, three values for axial induction can be obtained (1.1916, 0.76, 0.0483). The thrust coefficient for an ideal turbine is equal to zero when a=1.

On the other hand, the momentum theory is no longer valid at axial induction factors greater than 0.5, because V in the far wake would be negative. In practice, as the axial induction factor increases above 0.5, the flow patterns through the hydrokinetic turbine become much more complex than those predicted by the momentum theory. However, when axial induction is equal to a small value, the values of chord can be also smaller, generating

a decrease of the surface where the water acts, and complicating the structural integrity of the blade; therefore, the value of axial induction equal to 0.76 was used for the design of vertical-axis hydrokinetic turbine and was calculated using Equation. (8).

$$C_p = \frac{4a(1-a)^2}{\eta} \tag{8}$$

With the function defined in Equation. (7) and once C_L, C_D, a, and R have been found, it is possible to evaluate the chord length response at different values of azimuth angle (Figure 1). It is observed that the chord length change with azimuthal position and the distribution is cyclic every 180° with asymptotic values at 0° and 180°. For values of the azimuth angle between 0° and 60° and between 120° and 180°, the chord length is very large leading to chord length much larger than R. Therefore, in order to find an optimal value of chord length, the values of the chord length for the azimuth angles between 60° and 120° were averaged, obtaining a value equal to 0.33 m.

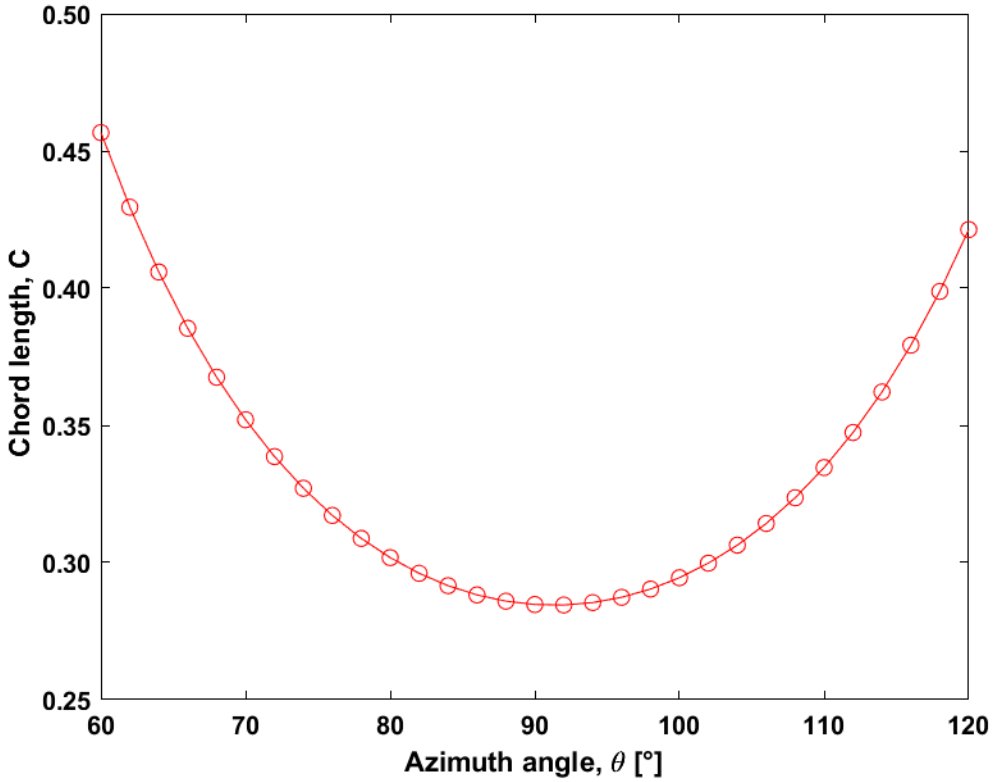

Figure 1. Chord length for different azimuth angles.

Using Equation. (4), σ of the turbine was possible to be found, obtaining a value of 0.66. A lower σ requires less material and more cost effectual. On the other hand, the blade aspect ratio (AB) is defined as the ratio of the blade length to its chord length [36]. It can be defined as expressed by Equation. (9).

$$AB = \frac{H}{C} \tag{9}$$

For blades with smaller aspect ratio, the lift to drag ratio can be reduced. Any decrease in lift to drag ratio will reduce tangential forces. This would decrease the turbine overall torque and, consequently, the turbine output power. Some researchers have demonstrated an increase in the maximum C_p with the blade AB up to the AB exceeds a value of about 15. In spite of this, utilizing blades with relatively high AB has some drawbacks. Relatively long blades add a great amount of weight to the turbine, which increases the manufacturing and maintenance costs and creates a need for a more complex bearing. Moreover, such blades are exposed to larger bending moments. In this work, the blade AB was 3.42.

After finding out the value of *C* for every section, the next step was to multiply these values by the non-dimensional coordinates of the *NACA 0025*. The values of *x* and *y* coordinates of the profile for each section were exported to parametric 3D design software. From the cross sections of the blade and using the Loft command, a 3D model of the whole blade could be produced. The resulting image is shown in Figure 2. In general, the geometric specifications of the turbine are given in Table 1.

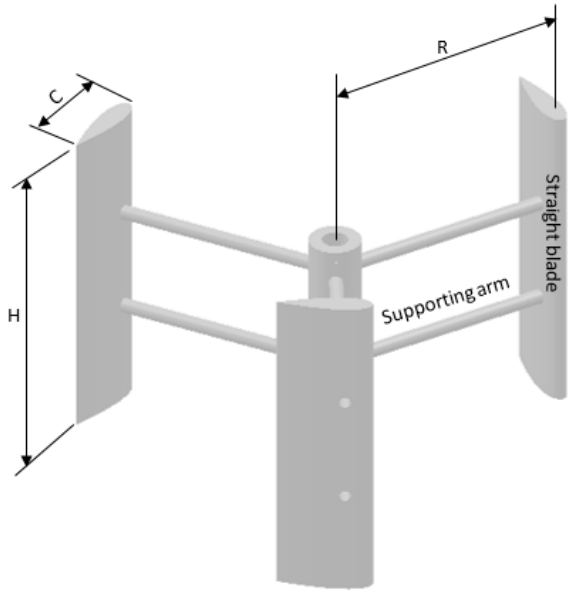

Figure 2. Darrieus vertical-axis hydrokinetic rotor with three blades.

Table 1. Geometric specifications of the turbine.

Parameter	**Value (units)**
Power output (P)	500 W
Blade´s profile	NACA 0025
Chord length (C)	0.33 m
Number of blade (N)	3
Solidity (σ)	0.66
Turbine height (H)	1.13 m
Turbine radius (R)	0.75 m

Numerical Model of the Vertical-axis Hydrokinetic Turbine

Three basic models are used for the modeling of a vertical-axis turbine. These models are: a) double multiple stream tube model, b) cascade model and c) vortex model. The first model devised to predict the efficiency is single stream tube model [39-42]. This model is based on the propeller disk theory, which assumes rotor as a solid rectangular disk on which induced velocities are constant and depend on drag. It is important to note that drag is an integral function of forces acting on the blades [43]. An improved version of this theory was proposed by dividing the disk into multiple cross-sections to take into account several V and α. The theory was further improved by dividing rotation in upstream and downstream [44-45]. Hirsch and Mansal [46] proposed the cascade model from the cascade theory. This theory is able to consider convergence problems of high σ and high TSR rotor by using the momentum model. 2D vortex models were proposed although they were limited to low TSR because of their incapability to take dynamic stall into account [47-48]. To improve this, Strickland et al., [49] developed a 3D model to consider dynamic stall. With the development of powerful computers, numerical analysis software are widely used for the design of this type of turbines. In this regard, CFD simulation is frequently used as an alternative to more expensive experimental studies in order to validate the performance of a turbine. The CFD package, Ansys Fluent version 18.0, was used for all the simulations performed in this study. Initial 2D CFD model with less computation cost that 3D model was used to represent the vertical hydrokinetic turbine and the water domain. Based on the review of relevant works [6, 50-52], it has been reported that a 2D model is sufficient in revealing the factors that influence the performance and majority of flow physics that surround the vertical-axis hydrokinetic turbine such as hydrofoil profile, N, σ, and D. In the 2D numerical study of this work, the effects from supporting arms were not taken into consideration. Unsteady Reynolds-Averaged Navier-Stokes (RANS) equations were solved using the SIMPLE algorithm for pressure velocity coupling [53-56].

The vertical hydrokinetic turbine studied was a 3-bladed Darrieus rotor with a NACA 0025 blade profile. C was set at 0.33 m with a rotor radius equal to 0.75 m. A central post with a D of 0.025 m was placed in the rotation axis. The mesh is a critical part of a CFD simulation for engineering purposes. It has to be coarse enough so that the calculation is affordable, but also fine enough so that each important physical phenomenon is captured and simulated. In this sense, the domain mesh was created around each hydrofoil and the surrounding water channel geometry was defined based on studies of the extents of the boundaries. There is an inner circular rotating domain connected to a stationary rectangular domain via a sliding interface boundary condition that conserves both mass and momentum. The domain extents were also selected from a series of sensitivity tests to determine the appropriate distance of the walls, inlet and outlet boundaries from the rotor of R. The domain extends 3 R upstream and 8 R downstream of the center of the turbine and 2.5 R laterally to either side of the turbine. The circular rotating domain has an overall diameter of 2.8 R. Because the computational domain is 2D, the turbine blades were implicitly assumed to be infinitely long.

Unstructured meshes were applied to both the rotor away from the near surface region and the outer grids. Finer meshes were used around the blades and regions in the wake of the blades. Particularly, regions at the leading edge, trailing edge and in the middle of blade were finely meshed in order to capture the flow field more accurately. The outer mesh was coarsened in regions expanding away from the rotor in order to minimize the central

processing unit (CPU) time. The different mesh zones used for the present simulations are illustrated in Figure 3, while various mesh details are shown in Figure 4a and 4b. A number of simulations were carried out in order to determine how the mesh quality was affecting the CFD results. In this sense, the torque was calculated for each grid using the Fluent solver. The objective was to select the most appropriate mesh that can guarantee low computational costs and good result accuracy. The quality of the mesh was also checked, as well as the y+ values around the blades, which is important for the turbulence modeling.

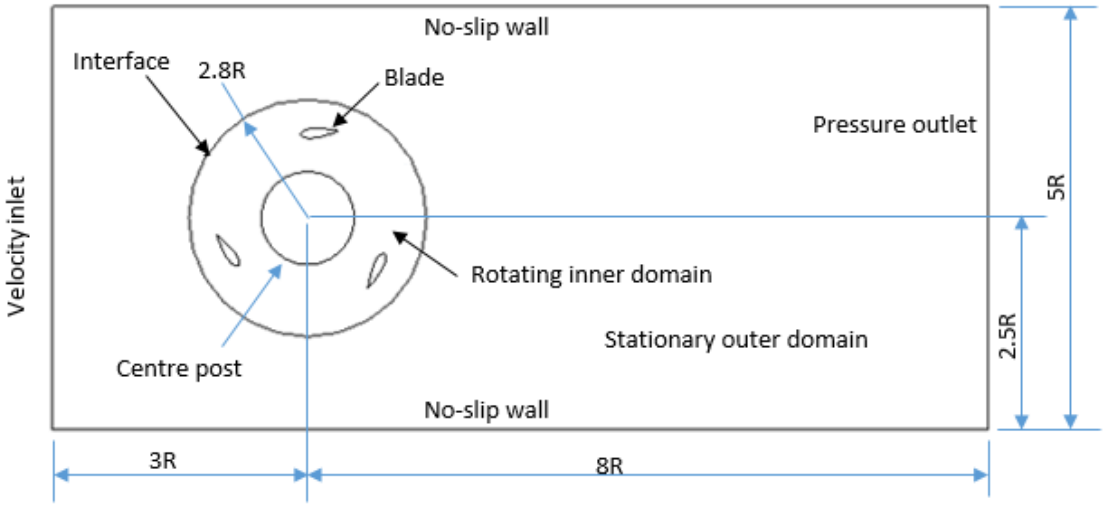

Figure 3. An illustration of the 2D numerical domain.

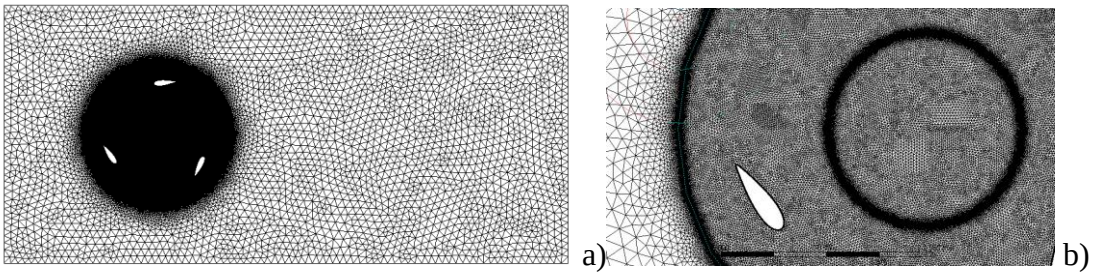

a) b)

Figure 4. (a) Detail of the mesh of the area around the blades. (b) Detail of the mesh of the rotor around the area of the interface.

Boundary conditions consist of two symmetry planes (top and bottom), a uniform pressure on the outlet boundary, and a uniform velocity on the inlet boundary with magnitude 1.5 m/s were used for the TSR and the corresponding ω shown in Table 2. k-ω Shear Stress Transport (SST) turbulence model was employed for turbulence modeling since it showed better performance for complex flows including adverse pressure gradients and flow separations like in vertical-axis hydrokinetic turbines. The no-slip boundary condition was applied on the turbine wall blades. To simulate the rotation of the rotor, the circular turbine mesh with embedded blades was allowed to move relative to the outer inertial fixed domain. An interface wall was introduced between the fixed and rotating domain. The origin of the

reference frame is the center of the rotor. The simulation methods used in this study is similar to methods used in other numerical studies. Here, the rotational speed of the turbine axis is specified by user input.

Table 2. Flow conditions in CFD Analysis.

λ	0.5	1	1.75	2	2.5
$\omega\ (rad/s)$	0.997	1.994	3.489	3.987	4.984

To solve the viscous sublayer of the k-ω turbulence model, the values of y+ generally must be less than 1. Subsequently, several meshes were made by increasing the refinement of the computational domain near the blade, achieving a good resolution of the boundary layer. The mesh 4 reached a convergence of results with 298878 nodes and 1.58% error on C_p (Table 3). In this way, further refinement might not improve the numerical results. The numerical results obtained from mesh 4 were compared with several results available in the literature.

Table 3. Mesh convergence study.

Mesh	**Nodes**	**y^+**	**Maximum power coefficient C_{pmax}**	**Error (%)**
Mesh 1	143672	0.246	0.56	10.71
Mesh 2	167896	0.221	0.64	14.28
Mesh 3	187630	0.283	0.63	1.56
Mesh 4	298878	0.261	0.62	1.58

Transient analyses are carried out to characterize the performance of the investigated profile NACA 0025. Performances are described in terms of the T and C_p, calculated according to Equation. (10). Due to the flow over Darrieus turbine is periodic, sufficient temporal resolution is necessary to ensure proper unsteady simulation of the vertical-axis hydrokinetic turbine and in order to ensure the solution is independent on the time step. Different time step sizes Δt that are equivalent to specific rotational displacements along the azimuth were tested. The chosen time step size was $\Delta t = 0.1°$, which properly captures the vortex shedding. Time step convergence was monitored for all conserved variables and it was observed that acceptable levels of residuals (less than 1×10^{-6}) were attained after 6 rotations of the hydrokinetic turbine. This meant that periodic convergence was also achieved.

$$C_P = \frac{P}{0.5\rho S_{ref} V^3} \tag{10}$$

On the other hand, turbine P and T fluctuation levels were simulated using transient time-accurate 3D numerical models utilizing ANSYS-Fluent version 18.0 in order to validate the rotor hydrodynamic design. The model included all the blades and shaft, which were meshed using unstructured elements. All dimensions of the boundary of domain (Figure 5) were given in terms of R. The width and length of the domain were chosen as 5 R and 11 R, respectively. The height of the domain was approximately 3 times R. The domain was made

large enough to capture the near wake and far wake effects. The study assumed unsteady and incompressible flow. The effect of the supporting arms and central shaft was not considered. The supporting arms affect the power output of a turbine by additional drag on the turbine. The velocity inlet boundary condition was applied on the left surface of the domain with uniform axial (free-stream) velocity of 1.5 m/s. A pressure outlet boundary condition was provided on the right surface with zero gauge pressure. The no-slip condition was applied on the turbine blade; i.e., the relative velocity of the surface blade was set to zero and k-ω SST turbulence model was also used [57, 58].

Mesh resolution was set by specifying the mesh size and growth rates to allow for local refinement of mesh zones. Mesh density was varied according to expected flow curvature rates resulting in increased mesh density in regions near the blades. In order to simulate the rotation of the turbine, an inner rotating domain was utilized with the interface placed between the stationary outer domain and the rotating inner domain, as shown in Figure 6, simulated as a transient rotor/stator using a GGI method. Turbine T was calculated using ANSYS CFX functions. A good quality CFD model design requires mesh refinement to achieve a grid-independent solution. Therefore, a mesh independent test was conducted by increasing the number of elements of the mesh until the turbine T did not experience hardly any variation by refining the mesh. Convergence was monitored by observing the residuals as well as T. Thus, the final mesh consisted of 368187 nodes. The CFD solutions were deemed to have converged when the scaled residuals for all solution values had dropped by at least six orders of magnitude. The moment on blade was monitored to ensure convergence of the solutions. Finally, the CFD simulations provided the flow field within the computational domain and also the blade pressure distribution.

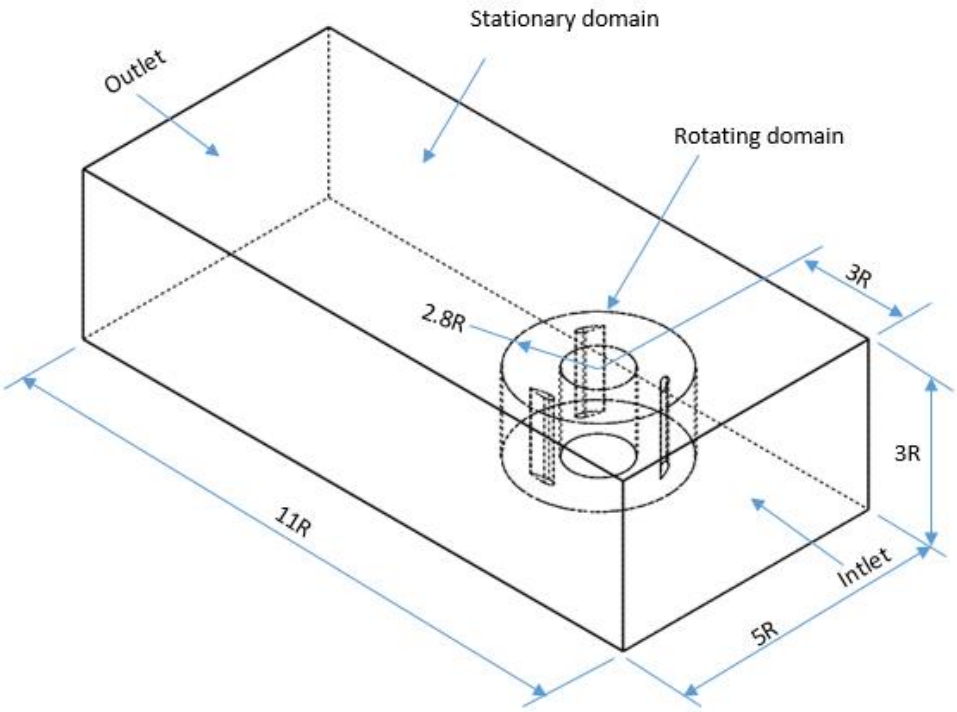

Figure 5. Computational domain used for CFD analysis.

Three geometrical configurations of the blade were studied using a 3D numerical model in order to choose the best configuration that causes less fluctuation in torque. The models are generated by using the SolidWorks CAD software. They are a straight-bladed Darrieus turbine with a D of 1.5 m. In model 1, the rotor consists of 3 blades with H equal to 1.13 m. Each blade is attached to a central shaft by two supporting arms. Model 2 consists of 6 blades with H equal to 0.565 m assembled on the axis into two groups. In both groups, the blades are 120° separated from each other, but each group has an offset angle of 60° from each other. Finally, model 3 has 9 blades with a H equal to 0.377 m, which are assembled into three groups on the axis. The separations between blades and groups are 120° and 60°, respectively. In Figure 6, the described configurations are illustrated.

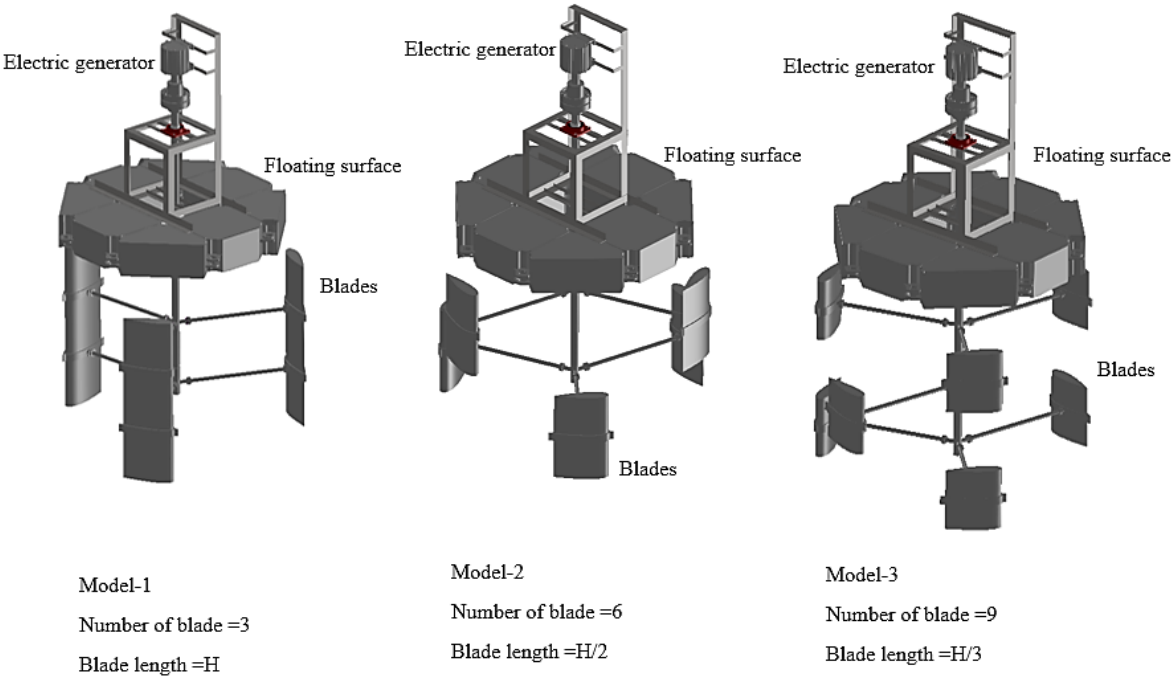

Figure 6. H-Darrieus vertical-axis hydrokinetic turbine.

RESULTS AND DISCUSSION

C_p variation over a range of TSR values was studied for the selection of the best TSR that led to optimum performance of profile NACA 0025, which was used in the blade geometrical design. The coefficient of performance versus azimuthal position of different TSR during rotation is shown in Figure 7. A nearly sinusoidal curve was obtained with three positive maxima at each turn and three positive minima (when TSR=1.75) or negative minima (when TSR = 0.50, 1.00, 2.00), meaning that during a revolution there are periods of time where the turbine produces torque on the fluid. Number of maxima at each turn was equal to N. It is observed that C_p increases approximately until 50° azimuthal position and decreases until 120° azimuthal position; i.e., the main power production occurs between 0° and 120° azimuthal position for the first blade when TSRs are 1.75 and 2.00. It can be seen that the maximum torque for the first blade is achieved at the azimuth angle around 50°. After the

peak, the drag begins to increase as the blade enters into a dynamic stall, and the drag starts to be dominant until an azimuth angle of 120°. Then, the second blade repeats the motion of the first blade and the power production is completed with the same motion of the third blade for one rotation of the turbine. Plot of C_p versus TSR shows positive values of TSR close to 1.75, meaning that fluid is providing torque to the turbine. Beyond TSR=1.75, C_p is negative, indicating that the turbine, rotating at a constant ω, exerts torque on the fluid. This can be explained because a high TSR implies a high turbine angular speed and, in such case, kinetic energy contained in flow is not enough to deliver torque to the turbine and makes it to rotate with the same ω.

In the literature, optimum values of TSR for a Darrieus turbine were reported. For example, Kiho et al. [59], using a Darrieus turbine diameter of 1.6 m, found that the highest efficiency achieved was 0.56 at 1.1 m/s V and 2 TSR. In turn, Torri et al. [60], also found that the peak C_p of a 3-blade straight vertical-axis hydrokinetic turbine was about 0.35 at a TSR of around 2. However, Dai et al., [38], performed numerical and experimental analyses with 4 sets of a 3-bladed rotor where blades were designed with NACA0025 with 4 different C. These 4 sets of rotors were tested in a tank at different flow velocities and radius. The highest C_p was achieved by the rotor with a C of 162.88 mm, R of 450 mm and TSR of 1.745. Furthermore, authors investigated the same rotor at different flow velocities and found 1.2 m/s as the most effective velocity. They concluded that larger rotors are more efficient while flow velocity has little effect on the turbine efficiency.

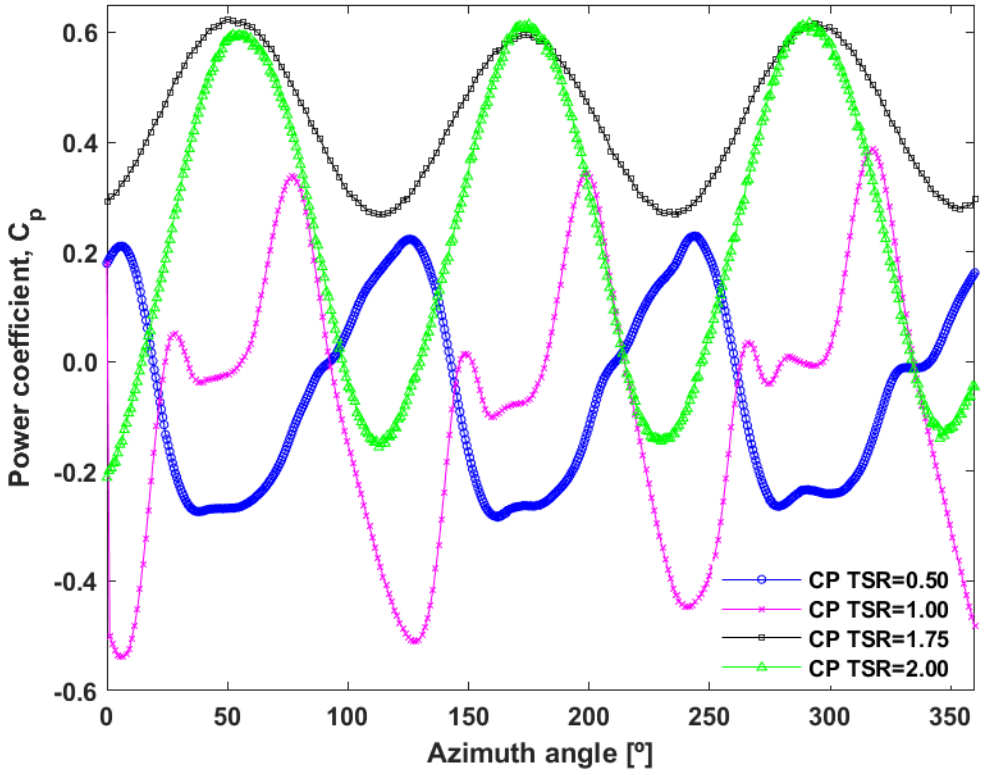

Figure 7. Variation of the power coefficient (C_p) with the azimuth angle (θ) for different tip speed ratios (TSR).

The same tendencies of C_p are found in the case of TSR of 1.75 and 2.00, as it can be seen in Figure 7. The amplitude of variation of C_p is lower when TRS is equal to 1.75. This result confirms that the blade with TSR of 1.75 has better performance than any other TSR. When TRS is equal to 1.75, the maximum average C_p is 0.62 and the amplitude of variation of C_p is near 0.37. On the other hand, when TSR is 2.00, the turbine achieved average torque coefficient near 0.61 and amplitude of only 0.83. Therefore, a turbine with a TRS of 1.75 has advantages over a turbine with a TRS of 2.00 in terms of the reduced fluctuation of its torque curve. C_p decreases for lower values of TSR because at low values of TSR, flow around blade is separated, implying low lift and high drag. As a result, transferred torque from fluid to turbine decreases. In general, the fluctuations in C_p and, therefore, in T can produce a high amount of vibration in the turbine. The effect of these vibrations directly influences the fatigue life of the turbine blades and that of the generated power**.**

On the other hand, the unsteady flow field is expected to be complex, particularly due to the wake effect. This effect can be seen from the velocity contour in Figure 8.

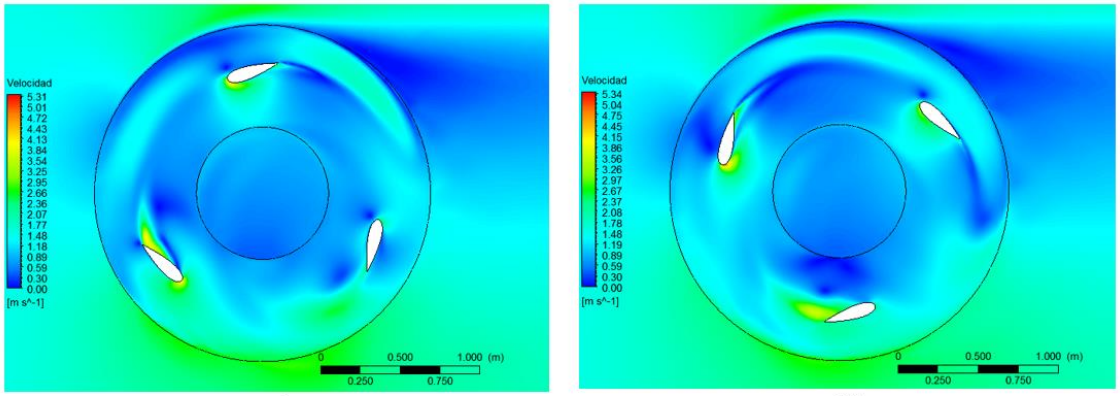

a) b)

Figure 8. Contour of velocity magnitude for rotor.
a) Azimuth angle = 0°, b) Azimuth angle = 30°.

As evidenced from Figure 8, the wake from the leading blade interacts with the following blade and velocity can reach a value even higher than 5.34 m/s. In order to perceive the effect of TSR on the turbine performance, the average powers achieved for different TSRs are depicted in Figure 9. The instantaneous C_p generated by the turbine is equal to the product of the turbine ω and T acting on it. C_p is not constant because the torque and velocity are not constant in the Darrieus turbine. Hence, the average C_p per cycle is calculated as the product of the average values of these terms per cycle.

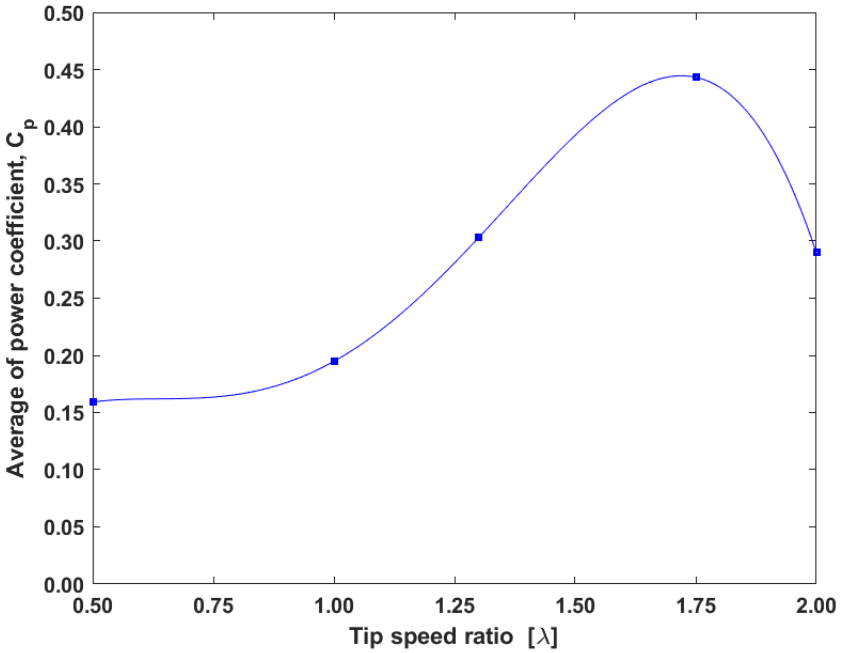

Figure 9. Average power coefficient (C_p) for different TSR.

According to the figure, TSR and C_p are in a direct relationship when the TSR is between 0.5 and 1.75. However, TSR and C_p have an opposite tendency for TSR greater than 1.75. The maximum value of the power was achieved when TSR was 1.75. Similar results were obtained by Dai et al. [61] for NACA0025 blade profile. Additionally, Lain and Osorio [60] used experimental data of Dai and Lam's work [61], and developed numerical models. They performed analysis on CFX solver, DMS model and Fluent solver, and achieved efficiencies of 58.6%, 46.3% and 52.8%, respectively, when TSR was 1.745. Results observed by using Fluent were quite accurate.

The results obtained from the 3D numerical analysis are presented in Figure 10. Many features can be concluded from this figure; firstly, by increasing the number of blades, the maximum C_p average increases. In the case of the turbine of model 1, the maximum C_p average is 0.24 and the amplitude of C_p variation, near 0.24. For model 2, the maximum C_p average is 0.51 and the amplitude of C_p variation, near 0.07. The turbine with 9 blades (model 3), represented in Figure 10, achieved average torque coefficient near 0.55 and amplitude of only 0.17. Model 2 have advantages over model 1 and 3 in terms of its reduced fluctuation of its torque curve.

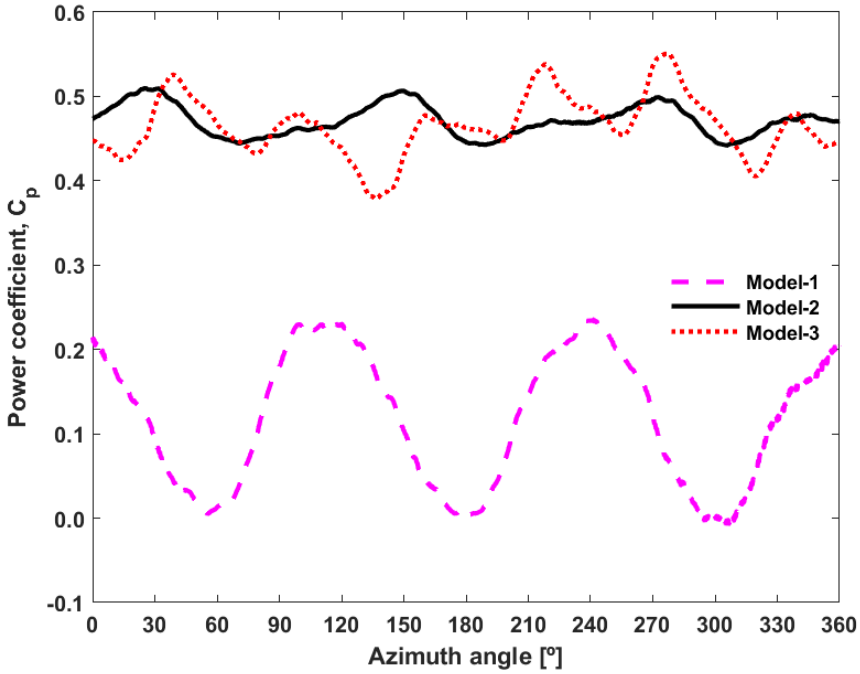

Figure 10. Power coefficient (C_p) curve comparing the fluctuation of Darrieus turbine with different geometric configurations.

Maitre et al. [63], using a modified Darrieus H-rotor with AR of 5.47 and TSR equal 2, found an experimental C_p equal to 0.34. In turn, Marsh et al. [64], using 3D transient CFD models of a 3 straight-bladed vertical-axis turbine in a commercial Unsteady Reynolds Averaged Navier–Stokes (URANS) solver and using a k-ω SST turbulence model, found that the maximum C_p value of about 0.25 was achieved at a TSR of 2. This value is similar to that obtained with model 1. The geometrical modifications (model 2 and model 3) made to the rotor in this work allow finding C_p values higher than those reported in the literature [2, 3 6]. The Darrieus straight bladed turbine, or H-Darrieus vertical-axis hydrokinetic turbine, was further examined by other researchers and the general conclusion was that this kind of turbines exhibits T fluctuations on the central transmitting shaft when the turbine is in operation. These fluctuations increase proportionally to the tip speed of the turbine exhibiting high amounts of vibration. The effect of these vibrations directly influenced the fatigue life of the turbine blades and that of the generated power [5, 6, 37, 38].

The configuration proposed in model 2 can reduce the fluctuation of the torque due to the increase in the number of blades [65, 66]. Thus by far, the utilization of helical blades is one of the most promising solutions to accomplish these goals [6, 7, 67]. However, the manufacture of the blade is more complicated, as stated previously. The blades of the model 2 are easy to be constructed and, therefore, this contributes to the minimization of the cost of energy of the hydrokinetic system.

CONCLUSION

The design and simulation of a vertical-axis hydrokinetic turbine were presented in this work. The numerical simulations allow analyzing many different turbine design parameters, providing an optimal configuration for a given set of design parameters.

The TRS is a significant parameter that affects the performance of hydrokinetic turbines. Consequently, the performance of the turbine was investigated with a simplified 2D and 3D numerical model. From the 2D model, C_p was computed for various TSR. During a turbine revolution, the blade of the turbine may experience large, as well as rapid variation, in C_p. A C_p maximum of 62% was achieved when TSR was equal to 1.75. On the other hand, using 3D transient CFD models of a 3 straight-bladed vertical-axis turbine in a commercial URANS solver and the k-ω SST turbulence model, the maximum C_p value was found to be about 0.55, 0.51 and 0.24 with model 3, 2 and 1, respectively. However, model 2 has advantages in comparison with model 1 and 3 in terms of the reduced fluctuation of its C_p curve.

In general terms, hydrokinetic turbine blades must be designed to convert the water kinetic energy into torque, while having structural properties that ensure the required static and fatigue strength for a long operational life. In addition, they must have low but enough material and reduced manufacturing costs so that the total hydrokinetic turbine system can be accepted by the final users. In this sense, model 2 seems to be promising for local electrical energy supply in developing countries, such that an operation in isolated networks is possible, due to this technology can be adopted easily and run efficiently with less environmental impact and less torque fluctuation.

ACKNOWLEDGMENTS

The authors gratefully acknowledge the financial support provided by the Colombia Scientific Program within the framework of the call Ecosistema Científico (Contract No. FP44842- 218-2018).

REFERENCES

[1] Anyi M, Kirke B. Evaluation of small axial ow hydrokinetic turbines for remote communities. Energy for Sustainable Development. 2010;14 (2):110-116.

[2] Kumar D, Sarkar S. A review on the technology, performance, design optimization, reliability, techno-economics and environmental impacts of hydrokinetic energy conversion systems. Renewable and Sustainable Energy Reviews. 2016;58:796-813.

[3] Vermaak HJ, Kusakana K, Koko SP. Status of micro-hydrokinetic river technology in rural applications: A review of literature. Renewable and Sustainable Energy Reviews. 2014;29:625-633.

[4] RH van Els, ACPB Junior. The brazilian experience with hydrokinetic turbines. Energy Procedia. 2015;75:259-264.

[5] Manwell JF, McGowan JG, Rogers AI. Aerodynamics of Wind Turbines. In: J.F Manwell, JG McGowan and AL Rogers (eds) Wind energy explained: theory, design and application. 2th ed. UK: John Wiley & Sons. 2009:91-155.
[6] Khan M, Bhuyan G, Iqbal M, Quaicoe J.E. Hydrokinetic energy conversion systems and assessment of horizontal and vertical axis turbines for river and tidal applications: A technology status review. Applied Energy. 2009;86(10):1823-1835.
[7] Chica E, Rubio-Clemente A. Design of Zero Head Turbines for Power Generation. In Renewable Hydropower Technologies. InTech, 2017:25-52.
[8] Güney M., Kaygusuz K. Hydrokinetic energy conversion systems: A technology status review. Renewable and Sustainable Energy Reviews. 2010;14(9):2996-3004.
[9] Beri H, Yao Y. Numerical simulation of unsteady flow to show self-starting of vertical axis wind turbine using fluent. Journal of Applied Sciences. 2011;11(6):962-970.
[10] Ali BR, Antonio CF. The effect of inertia and flap on autorotation applied for hydrokinetic energy harvesting. Applied Energy. 2015;143: 312-323.
[11] Gorlov AM. Helical turbines for the gulf stream: Conceptual approach to design of a large-scale floating power farm. Marine Technology. 1998;35(3):175-182.
[12] Sahim K, Santoso D, Radentan A. Performance of combined water turbine with semielliptic section of the savonius rotor. International Journal of Rotating Machinery. 2013;985943:1-5.
[13] Kamal ARI, Tiago PB. A comparative study on river hydrokinetic turbine blade profiles. Journal of Engineering Research and Application. 2015;5(5):1-10.
[14] Khan NI, Iqbal T, Hinchey M, Masek V. Performance of Savonius rotor as a water current turbine. The Journal of Ocean Technology. 2009;4(2):72–83.
[15] Gorban AN, Gorlov AM, Silantyev VM. Limits of the turbine efficiency for free fluid flow. Journal of Energy Resources Technology. 2001;123(4):311–7.
[16] Golecha K, Eldho TI, Prabhu SV. Influence of the deflector plate on the performance of modified Savonius water turbine. Applied Energy. 2011;88(9):3207-3217.
[17] Guang ZHO, Yang RS, Yan IU, Zhao PF. Hydrodynamic performance of a vertical-axis tidal-current turbine with different preset angles of attack. Journal of Hydrodynamics, Ser. B. 2013;25(2):280-287.
[18] Bachant P, Wosnik M. Performance measurements of cylindrical- and spherical-helical cross-flow marine hydrokinetic turbines, with estimates of exergy efficiency. Renewable Energy. 2015;74:318–325.
[19] Malipeddi AR, Chatterjee D. Influence of duct geometry on the performance of Darrieus hydroturbine. Renewable Energy. 2012;43:292-300.
[20] Tanaka K, Hirowatari K, Shimokawa K, Watanabe S, Matsushita D, Furukawa, A. A Study on Darrieus-type Hydroturbine toward Utilization of Extra-Low Head Natural Flow Streams. International Journal of Fluid Machinery and Systems. 2013;6(3):152-159.
[21] Kirke B. Tests on two small variables pitch cross flow hydrokinetic turbines. Energy for Sustainable Development. 2016;31:185-193.
[22] Bachant P, Wosnik M, Gunawan B, Neary V.S. Experimental study of a reference model vertical-axis cross-flow turbine. PloS one. 2016;11(9):e0163799.

[23] Bachan P, Wosnik M. Effects of Reynolds number on the energy conversion and near-wake dynamics of a high solidity vertical-axis cross-flow turbine. Energies. 2016;9(2):73

[24] Gorle JMR, Chatellier L, Pons F, Ba M. Flow and performance analysis of H-Darrieus hydroturbine in a confined flow: A computational and experimental study. Journal of Fluids and Structures. 2016;66:382-402.

[25] Gosselin R, Dumas G, Boudreau M. Parametric study of H-Darrieus vertical-axis turbines using CFD simulations. Journal of Renewable and Sustainable Energy. 2016; 8(5):053301.

[26] Patel V, Eldho TI, Prabhu V. Experimental investigations on Darrieus straight blade turbine for tidal current application and parametric optimization for hydro farm arrangement. International Journal of Marine Energy. 2017,17:110-135.

[27] Somoano M, Huera-Huarte F. Flow dynamics inside the rotor of a three straight bladed cross-flow turbine. Applied Ocean Research. 2017;69:138-147.

[28] Somoano M, Huera-Huarte, F. The effect of blade pitch on the flow dynamics inside the rotor of a three-straight-bladed cross-flow turbine. Proceedings of the Institution of Mechanical Engineers, Part M: Journal of Engineering for the Maritime Environment. 2018;0(0):1-11.

[29] Naitik P, Mohammad H, Vishal M. Experimental performance of darrieus hydro turbine. International Journal of Advance Engineering and Research Development. 2018;5(6):431-436.

[30] Patel V, Eldho TI, Prabhu SV. Performance enhancement of a Darrieus hydrokinetic turbine with the blocking of a specific flow region for optimum use of hydropower. Renewable Energy. 2019;135:1144-1156.

[31] Biadgo MA, Simonovic A, Komarov D, Stupar S. Numerical and Analytical Investigation of Vertical Axis Wind Turbine. FME Transactions. 2013;41:49-58.

[32] Chica E, Pérez F, Rubio-Clemente A. Rotor structural design of a hydrokinetic turbine. International Journal of Applied Engineering Research. 2016;11(4):2890-2897.

[33] Anyi M, Kirke B. Hydrokinetic turbine blades: Design and local construction techniques for remote communities. Energy for Sustainable Development. 2011;15(3): 223-230.

[34] Hagerman G, Polagye B, Bedard R, Previsic M. Methodology for estimating tidal current energy resources and power production by tidal in-stream energy conversion (TISEC) devices. Rep. EPRI-TP-001 NA Rev 2, Electr. Power Res. Inst., Palo Alto, CA. 2006:1-57.

[35] Robert E, Sheldahl P, Klimas C. Aerodynamic characteristics of seven symmetrical airfoil sections through 180-degree angle of attack for use in aerodynamic analysis of vertical axis wind turbines. SAND80-2114. Unlimited Release. Sandia National Laboratories, 1981.

[36] Mohamed MH. Performance investigation of H-rotor darrieus turbine with new airfoil shapes. Energy. 2012;47(1):522-530.

[37] Mojtaba AB, Rupp C, David SKT. Straight-bladed vertical axis wind turbine rotor design guide based on aerodynamic performance and loading analysis. Proceedings of the Institution of Mechanical Engineers, Part A: Journal of Power and Energy. 2014; 228(7):742 – 759.

[38] Dai, YM, Lam W. Numerical study of straight-bladed Darrieus type tidal turbine. ICE-Energy. 2009;162:67-76.
[39] Brahimi MT, Allet A, Paraschivoiu I. Aerodynamic analysis models for vertical-axis wind turbines. International Journal of Rotating Machinery. 1995;2(1):15-21.
[40] Islam M, Ting DSK, Fartaj A. Aerodynamic models for Darrieus-type straight-bladed vertical axis wind turbines. Renewable and Sustainable Energy Reviews. 2008; 12(4):1087-1109.
[41] Paraschivoiu I, Saeed F, Desobry V. Prediction capabilities in vertical-axis wind turbine aerodynamics. In The World Wind Energy Conference and Exhibition, Berlin, 2002:2-6.
[42] Paraschivoiu I. Wind turbine design: with emphasis on Darrieus concept. Polytechnic International Press,. Montreal, Québec, Canada. 2002: 438.
[43] Templin R.J. Aerodynamic performance theory for the NRC vertical-axis wind turbine. NASA STI/Recon Technical Report N, 1974;76.
[44] Strickland JH. Darrieus turbine: a performance prediction model using multiple streamtubes. (No. SAND-75-0431). Sandia Labs., Albuquerque, N. Mex.(USA), 1975.
[45] Paraschivoiu I. Double-multiple streamtube model for studying vertical-axis wind turbines. Journal of Propulsion and Power. 1988;4(4):370-377.
[46] Hirsch IH, Mandal AC. A cascade theory for the aerodynamic performance of Darrieus wind turbines. Wind Engineering. 1987:164-175.
[47] Holme O. A contribution to the aerodynamic theory of the vertical-axis wind turbine. In International Symposium on Wind Energy Systems. 1977:54-55.
[48] Fanucci JB, Walters R.E. Innovative wind machines: the theoretical performance of a vertical-axis wind turbine. In Proc. Of the VAWT Technology Workshop, Sandia Lab. Report SAND, 1976:5576-5586.
[49] Strickland JH, Webster B.T, Nguyen T. A vortex model of the Darrieus turbine: an analytical and experimental study. Journal of Fluids Engineering. 1979;101(4):500-505.
[50] Carrigan TJ, Dennis BH, Han Z.X, Wang BoP. Aerodynamic shape optimization of a vertical-axis wind turbine using differential evolution. ISRN Renewable Energy. 2012; Article ID 528418:1-16.
[51] Ghatage SV, Joshi JB. Optimisation of vertical axis wind turbine: CFD simulations and experimental measurements. The Canadian Journal of Chemical Engineering. 2011;90(5):1186-1201.
[52] Sabaeifard P, Razzaghi H, Forouzandeh A. Determination of vertical axis wind turbines optimal configuration through CFD simulations. In: International Conference on Future Environment and Energy, Singapore 22-25 February 2012:109-113.
[53] Jung HJ, Lee JH, Rhee SH, Song M, Hyun B-S. Unsteady flow around a two-dimensional section of a vertical axis turbine for tidal stream energy conversion. International Journal of Naval Architecture and Ocean Engineering, 2009;1(2):64-69.
[54] Islam M, Ting DSK, Fartaj A. Aerodynamic models for Darrieus-type straight-bladed vertical axis wind turbines. Renewable and Sustainable Energy Reviews. 2008;2(4):1087-1109.

[55] Raciti CM, Englaro A, Benini E. The Darrieus wind turbine: proposal for a new performance prediction model based on CFD. Energy. 2011;36(8):4919-4934.

[56] Dai YM, Gardiner N, Sutton R, Dyson PK. Hydrodynamic analysis models for the design of Darrieus-type vertical-axis marine current turbines. Part M, Journal of Engineering for the Maritime Environment. 2011;225:295-307.

[57] Ashwindran S, Azizuddin AA, Oumer AN. Computational fluid dynamic (CFD) of vertical-axis wind turbine: mesh and time-step sensitivity study. Journal of Mechanical Engineering and Sciences. 2019; 13(3):5604-5624.

[58] Septyaningrum E, Hantoro R, Utama IKAP, Prananda J, Nugroho G, Mahmasani A.W, Satwika NA. Performance analysis of multi-row vertical axis hydrokinetic turbine–straight blade cascaded (VAHT-SBC) turbines array. Journal of Mechanical Engineering and Sciences. 2019;13(3):5665-5688.[59] Kiho S, Shiono M, Suzuki K. The power generation from tidal currents by Darrieus turbine. Renewable energy. 1996;9(1-4):1242-1245.

[60] Torii T, Ookubo H, Yamane M, Sagara K, Seki K, Sekita K. A study on effectiveness of straight-wing vertical-axis hydro turbine generation system in the tidal current. In The seventeenth international offshore and polar engineering conference. International Society of Offshore and Polar Engineers 2007, 1-6 July, Lisbon, Portugal.

[61] Dai Y.M, Lam W. Numerical study of straight-bladed Darrieus-type tidal turbine. Proceedings of the Institution of Civil Engineers-Energy. 2009;162(2):67-76.

[62] Lain S, Osorio C. Simulation and evaluation of a straight-bladed Darrieus-type cross flow marine turbine. Journal of Scientific & Industrial Research. 2010;69:906-912.

[63] Maître T, Amet E, Pellone C. Modeling of the flow in a Darrieus water turbine: Wall grid refinement analysis and comparison with experiments. Renewable Energy. 2013;51: 497-512.

[64] Marsh P, Ranmuthugala D, Penesis I, Thomas G. Three-dimensional numerical simulations of straight-bladed vertical axis tidal turbines investigating power output, torque ripple and mounting forces. Renewable Energy. 2015;83:67-77.

[65] Castelli MR, Betta SD, Benini E. Proposal of a means for reducing the torque variation on a vertical axis water turbine by increasing the blade number. International Journal of Engineering and Applied Sciences. 2012;6:221-227.

[66] Hwang IS, Lee YH, Kim SJ. Optimization of cycloidal water turbine and the performance improvement by individual blade control. Applied Energy. 2009;86(9):1532-1540.

[67] Shiono M, Suzuki K, Kiho S. Output characteristics of darrieus water turbine with helical blades for tidal current generations. In: Proceedings of The Twelfth (2002) International Offshore and Polar Engineering Conference, Kitakyushum, Japan, 26-31 May 2002, 859-864.